Annals of Pure and Applied Mathematics
Vol. 3, No.2, 2013, 189-200
ISSN: 2279-087X (P), 2279-0888(online)
Published on 13 September 2013
www.researchmathsci.org

Annals of
Pure and Applied Mathematics

Hall Current Effects on Magnetohydrodynamics Fluid over an Infinite Rotating Vertical Porous Plate Embedded in Unsteady Laminar Flow

Nisat Nowroz Anika[1], Md. Mainul Hoque[2,*] and Nazmul Islam[3]

[1,3]Mathematics Discipline, Science, Engineering and Technology School
Khulna University, Khulna-9208, Bangladesh
[2,*]Department of Chemical Engineering, The University of Newcastle
NSW-2308, Australia

[*]Corresponding Email: mohammadmainul.hoque@uon.edu.au

Received 4 September 2013; accepted 11 September2013

Abstract. This work is concerned with the Numerical treatment of MHD on unsteady Magnetohydrodynamics Fluid flow past an infinite rotating vertical porous plate with heat transfer considering Hall current has been made. The solution would be based mainly on numerical transformation methods. The above mentioned framework has been considered in the one-dimensional unsteady problem. The system of equations has been transformed by usual transformation into a non-dimensional form. The dimensionless momentum and temperature equations are solved numerically by implicit finite difference technique. They are discussed for different time steps as well as for different values of parameters of physical and engineering interest. Also the corresponding wall shear stresses as well as rate of heat transfer coefficient, better named the Nusselt number has been performed. The obtained solutions have been graphically represented for different values of the well-known parameters. Finally, a qualitative comparison has been made between the present work and previous published result.

Keywords: MHD, Heat transfer, Implicit Finite difference, Hall Current

AMS Mathematics Subject Classification (2010): 35Q35, 37N10

1. Introduction

MHD flow problems have become in view of its significant applications in industrial manufacturing processes such as plasma studies, petroleum industries Magnetohydrodynamics power generator cooling of clear reactors, boundary layer control in aerodynamics. Many authors have studied the effects of magnetic field on mixed, natural and force convection heat and mass transfer problems. Indeed, MHD laminar boundary layer behaviour over a stretching surface is a significant type of flow having considerable practical applications in chemical engineering, electrochemistry and polymer processing. This problem has also an important bearing on metallurgy where magnetohydrodynamic (MHD) techniques have recently been used.

Chin et al. [6] obtained numerical results for the steady mixed convection boundary layer flow over a vertical impermeable surface embedded in a porous medium when the viscosity of the fluid varies inversely as a linear function of the temperature. Pal and Talukdar [5] analysed the combined effect of mixed convection with thermal radiation and chemical reaction on MHD flow of viscous and electrically conducting fluid past a vertical permeable surface embedded in a porous medium is analysed. Mukhopadhyay [8] performed an analysis to investigate the effects of thermal radiation on unsteady mixed convection flow and heat transfer over a porous stretching surface in porous medium. Hayat et al. [9] analysed a mathematical model in order to study the heat and mass transfer characteristics in mixed convection boundary layer flow about a linearly stretching vertical surface in a porous medium filled with a viscoelastic fluid, by taking into account the diffusionthermo (Dufour) and thermal-diffusion (Soret) effects.

Abdelkhalek [2] investigated the effects of mass transfer on steady two dimensional laminar MHD mixed convection flow. Crane [4] considered the problem of steady 2D, incompressible MHD flow past a circular cylinder with an applied magnetic field parallel to the main flow. Chowdhury and Islam [3] presented a theoretical analysis of a MHD free convection flow of a viscoelastic fluid adjacent to a vertical porous plate. Abo-Eldahab and Elbarbary [1] studied the Hall current effects on MHD free-convection flow past a semi-infinite vertical plate with mass transfer. The effect of Hall current on the steady magnetohydrodynamics flow of an electrically conducting, incompressible Burger's fluid between two parallel electrically insulating infinite planes was studied by Rana et al. [7].

Hence our aim is to study the roll of magnetic field on ionized Magnetohydrodynamics fluid flow through an infinite rotating vertical porous plate with heat transfer. The investigation has been made for solving the system of nonlinear equations. For this purpose the implicit finite difference technique has been used for problems for which non-similar solutions of the coupled non-linear partial differential equations are sought. Therefore, it is necessary to investigate in detail the distributions of primary velocity, secondary velocity and temperature across the boundary layer in addition to the Suction parameter. Also the Shear stresses as well as Nusselt number follows their usual trends.

2. Mathematical Model of the Flow

Consider an unsteady laminar, incompressible, viscous as well as electrically conducting fluid flowing through an infinite vertical porous plate. Initially the flow velocity patternU_∞, density ρ_∞ and temperature $T_\infty$are assumed to be uniform which is similar to that of fluid outside from the boundary layer. In Fig. 1(a) the $x-$axis is taken along the vertical plate with usual porosity. And y-axis is normal to the plate. The flow is permitted by a non-conducting vertical porous plate which is taken along $x-$axis in the upward direction. The unsteady fluid flow starts at $t = 0$, afterward the whole frame is allowed to rotate with an angular velocity R about y-axis. With $t > 0$, the porous plate is started to move in its own plane with constant velocity U_0 and with this also rises or fall its temperature from T_w to T_∞ instantaneously which is thereafter be maintained as such.

A strong uniform magnetic field of strength $B_0$is applied normal to the plate which is electrically non-conducting that induced another magnetic field on the electrically conducting fluid. Here we assumed that, $\boldsymbol{B} = (0, B_0, 0)$ and the magnetic lines of force are fixed relative to that of fluid. In general, the electrically conducting fluid is affected by Hall current in the presence of strong magnetic field. Consequently, the effect of Hall current gave rise to a force in the z-direction. Eventually it permitted a cross flow in the z-direction. Therefore, the flow becomes two dimensional. Since the plate is of infinite extent and also the motion of the fluid is unsteady, therefore, all the flow variables are depend on y and time t.

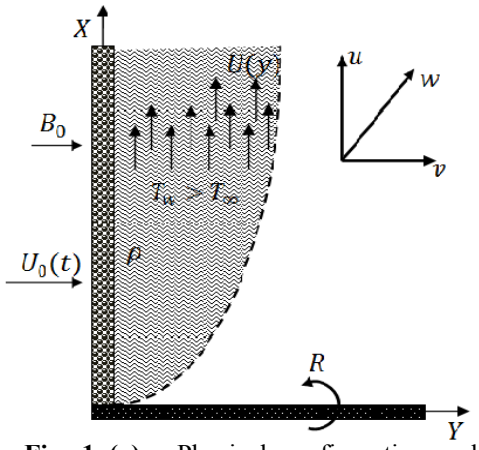

Fig. 1 (a): Physical configuration and Co-ordinate system.

From continuity equation, v_0 represents the constant suction velocity. The equation of conservation of charge $\nabla . J = 0$ gives $J_y = \text{constant}$. Since the direction of propagation only along the y-axis $\boldsymbol{J}$does not have any variation in $y-$direction. This constant is zero and hence $J_y = 0$ at the plate and consequently zero everywhere. In this case, the generalized Ohm's law should be in another form. Considered as;

$$\frac{m_e}{e^2 n}\frac{\partial \vec{J}}{\partial t} = \vec{E} + \vec{q} \wedge \vec{B} - \frac{\vec{J} \wedge \vec{B}}{en} + \frac{\nabla \rho_e}{en} - \frac{\vec{J}}{\sigma_e} \tag{1}$$

Here, 1st term in the left hand side reefers to current acceleration, 3rd term on the right hand side denoted that the Hall effect (owing to Lorentz Force) and the following term on the right hand side stands for diffusive streaming caused by the pressure gradient. Thus accordance with the above framework and Boussinesq's approximation, the basic boundary layer equations are given by,

Momentum equation in x-direction with rotation, thermal buoyancy force and Hall current;

$$\frac{\partial u}{\partial t} - v_0 \frac{\partial u}{\partial y} = \vartheta \left(\frac{\partial^2 u}{\partial y^2}\right) + g\beta(T - T_\infty) + 2Rw - \frac{B_0^2 \sigma_e}{\rho(1 + m^2)}(u + mw) \tag{2}$$

Momentum equation in z-direction with rotation and Hall current;

$$\frac{\partial w}{\partial t} - v_0 \frac{\partial w}{\partial y} = \vartheta \left(\frac{\partial^2 w}{\partial y^2}\right) - 2Ru + \frac{B_0^2 \sigma_e}{\rho(1 + m^2)}(mu - w) \tag{3}$$

Energy equation with viscous dissipation and Joule's dissipation;

$$\frac{\partial T}{\partial t} - v_0 \frac{\partial T}{\partial y} = \frac{\kappa}{\rho c_p}\frac{\partial^2 T}{\partial y^2} + \frac{1}{c_p}\vartheta\left[\left(\frac{\partial u}{\partial y}\right)^2 + \left(\frac{\partial w}{\partial y}\right)^2\right] + \frac{\sigma_e {B_0}^2}{\rho c_p (1 + m^2)}(u^2 + w^2) \tag{4}$$

with the boundary conditions for the present problem are given by,

$$\begin{aligned} &u = U_0, \quad w = 0, \quad T = T_w \text{at } y = 0 \text{ and } t > 0 \\ &u = 0, \quad w = 0, \quad T \to T_\infty \text{as } y \to \infty \text{ and } t > 0 \end{aligned} \tag{5}$$

where u, w are the velocity components in the x, z direction respectively, g is the acceleration due to gravity, β is the coefficient of volume expansion, T and T_∞ are the temperature of the fluid inside the thermal boundary layer and the fluid temperature in the free stream, respectively. $\vartheta$is the kinematic viscosity, ρ be the density, σ_e is the electrical conductivity, B_0 be the strength of the magnetic field, m is the Hall current, where, $m = \sigma_e B_0/en$. $\kappa$is the thermal conductivity of the medium, c_p is the specific heat at constant pressure.$e$be the electron charge and n represents number density of electron.

3. Mathematical Formulation

Mathematical formulation of this problem is dimensionalised by usual transformation technique. For this the required problem is introduced the following dimensionless variables to attain the solution of non-linear coupled partial differential equations.

$$Y = \frac{yU_0}{\vartheta}, \qquad U = \frac{u}{U_0}, \qquad W = \frac{w}{U_0}, \qquad \tau = \frac{t{U_0}^2}{\vartheta}, \qquad \theta = \frac{T - T_\infty}{T_w - T_\infty}$$

Applying all these non-dimensional variables into the equation (2) to (4), the basic equations relevant to the problem are in dimensionless form, as;

$$\frac{\partial U}{\partial \tau} - \epsilon \frac{\partial U}{\partial Y} = \frac{\partial^2 U}{\partial Y^2} + G_r\theta + 2\Gamma W - \frac{\mathrm{M}}{(1+m^2)}(u + mw) \tag{6}$$

$$\text{Similarly} \frac{\partial W}{\partial \tau} - \epsilon \frac{\partial W}{\partial Y} = \frac{\partial^2 W}{\partial Y^2} - 2\Gamma U + \frac{\mathrm{M}}{(1+m^2)}(mu - w) \tag{7}$$

$$\frac{\partial \theta}{\partial \tau} - \epsilon \frac{\partial \theta}{\partial Y} = \frac{1}{P_r}\frac{\partial^2 \theta}{\partial Y^2} + E_c\left[\left(\frac{\partial U}{\partial Y}\right)^2 + \left(\frac{\partial W}{\partial Y}\right)^2\right] + \mathrm{M}\frac{E_c}{(1+m^2)}(U^2 + W^2) \tag{8}$$

with the corresponding boundary conditions

$$\tau > 0, \quad \begin{matrix} U = 1, \ W = 0, \quad \theta = 1 & \text{at } Y = 0 \\ U = 0, \ W = 0, \quad \theta = 0 & \text{as } Y \to \infty \end{matrix} \tag{9}$$

where, $\epsilon = \frac{\mathrm{v}_0}{\mathrm{U}_0}$(Suction parameter), $G_r = \frac{g\beta(T_w - T_\infty)\sigma^2}{U_0\vartheta}$(Grashof Number),

$\mathrm{M} = \frac{\sigma_e {B_0}^2 \sigma^2}{\rho\vartheta}$(Magnetic Parameter), $P_r = \frac{\rho c_p \vartheta}{\kappa}$(Prandlt Number),

$\Gamma = \frac{R\vartheta}{U_0^2}$(Rotation pa), $m = \frac{\sigma_e B_0}{en}$(Hall Current), $E_c = \frac{{U_0}^2}{c_p(T_w - T_\infty)}$(Eckert Number).

4. Method of Solution

Systems of non-linear coupled partial differential equations with the boundary conditions are very difficult to solve analytically. For simplicity the implicit finite difference method has been used to solve (6) to (8) subject to the boundary conditions (9). In this case the region within the boundary layer is divided by some perpendicular lines of Y- axis, where Y- axis is normal to the medium as shown in Fig. 1(b).

It should be noted that the maximum length of boundary layer is $Y_{max}(= 35)$ as corresponds to $Y \to \infty$ i.e. Yvaries from 0 to 35. And the number of grid spacing in Y directions is $m(= 200)$, hence the constant mesh size along Y axis becomes $\Delta Y = 0.175\ (0 \le Y \le 35)$ with the smaller time step $\Delta\tau = 0.001$.

Using the finite difference method, U, W, and θ can be represented in terms of the values of $U_i^n, W_i^n,$ andθ_i^n at the end of the time step respectively. Implicit finite difference approximation gives;

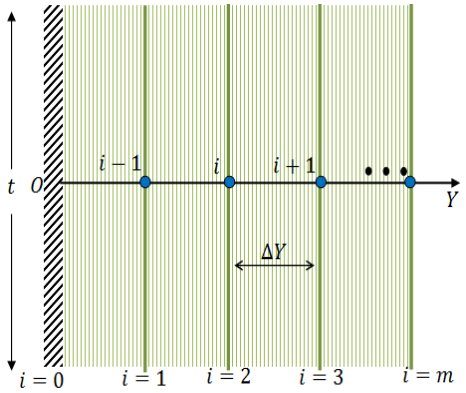

Fig. 1(b): Implicit finite difference space grid.

$$\left(\frac{\partial U}{\partial \tau}\right)_i = \frac{U_i^{n+1} - U_i^n}{\Delta\tau}, \left(\frac{\partial U}{\partial Y}\right)_i = \frac{U_{i+1}^n - U_i^n}{\Delta Y}, \left(\frac{\partial^2 U}{\partial Y^2}\right)_i = \frac{U_{i+1}^n - 2U_i^n + U_{i-1}^n}{(\Delta Y)^2}$$

$$\left(\frac{\partial W}{\partial \tau}\right)_i = \frac{W_i^{n+1} - W_i^n}{\Delta\tau}, \left(\frac{\partial W}{\partial Y}\right)_i = \frac{W_{i+1}^n - W_i^n}{\Delta Y}, \left(\frac{\partial^2 W}{\partial Y^2}\right)_i = \frac{W_{i+1}^n - 2W_i^n + W_{i-1}^n}{(\Delta Y)^2}$$

$$\left(\frac{\partial \theta}{\partial \tau}\right)_i = \frac{\theta_i^{n+1} - \theta_i^n}{\Delta\tau}, \left(\frac{\partial \theta}{\partial Y}\right)_i = \frac{\theta_{i+1}^n - \theta_i^n}{\Delta Y}, \quad \left(\frac{\partial^2 \theta}{\partial Y^2}\right)_i = \frac{\theta_{i+1}^n - 2\theta_i^n + \theta_{i-1}^n}{(\Delta Y)^2}$$

Substituting the above relations into the corresponding partial differential equation (6) to(8), an appropriate set of finite difference equations have been made as

$$\frac{U_i^{n+1} - U_i^n}{\Delta\tau} - \epsilon \frac{U_{i+1}^n - U_i^n}{\Delta Y} \frac{U_{i+1}^n - 2U_i^n + U_{i-1}^n}{(\Delta Y)^2} + G_r\theta_i^n + 2\Gamma W_i^n - \frac{M}{(1+m^2)}(U_i^n + mW_i^n) \quad (10)$$

$$\frac{W_i^{n+1} - W_i^n}{\Delta\tau} - \epsilon \frac{W_{i+1}^n - W_i^n}{\Delta Y} = \frac{W_{i+1}^n - 2W_i^n + W_{i-1}^n}{(\Delta Y)^2} - 2\Gamma U_i^n + \frac{\mathrm{M}}{(1+m^2)}(mU_i^n - W_i^n) \quad (11)$$

$$\frac{\theta_i^{n+1} - \theta_i^n}{\Delta\tau} - \epsilon \frac{\theta_{i+1}^n - \theta_i^n}{\Delta Y} = \frac{1}{P_r} \frac{\theta_{i+1}^n - 2\theta_i^n + \theta_{i-1}^n}{(\Delta Y)^2} + E_c \left[\left(\frac{U_{i+1}^n - U_i^n}{\Delta Y}\right)^2 + \left(\frac{W_{i+1}^n - W_i^n}{\Delta Y}\right)^2\right]$$

$$+\mathrm{M}\frac{E_c}{\left(\alpha_e{}^2 + \beta_e{}^2\right)}\left(U_i^{n2} + W_i^{n2}\right) \quad (12)$$

and the boundary condition with finite difference scheme as;

$$\begin{aligned} U_0^n = 1, \quad W_0^n = 0, \quad \theta_0^n = 1, \quad & \tau > 0 \\ U_L^n = 0, \quad W_L^n = 0, \quad \theta_L^n = 0, \quad & \tau > 0 \end{aligned} \quad (13)$$

Here the subscript i degenerate the grid points with Y coordinates and superscript n represents a value of time, $\tau = n\Delta\tau$, where, $n = 0,1,2,3, \ldots\ldots\ldots\ldots$ At the end of any time step $\Delta\tau$, the new temperature θ_i^{n+1}, the new secondary velocity W_i^{n+1}, and the new primary velocity U_i^{n+1} at all interior nodal points, may be obtained by successive applications of (10) to (12) respectively. Also the numerical values of the shear stresses, as well as Nusselt number are eventually by five point approximate formula for the derivatives. But the overall criteria are not shown for brevity.

5. Results and discussion

This Framework is plotted within the intermediate region of thermal boundary layer for different values of dimensionless suction parameter(S), the magnetic parameter (M), Hall current (m), Prandtl number (P_r), Grashof number (G_r), Rotation Parameter (Γ) and Eckert number (E_c). The values of Grashof number G_r are varied with positive and negative numbers; this problem refers to the values of $G_r > 0$ as grater cooling and greater heating respectively. Also the results are limited to $P_r = 0.71$ (Prandtl number for air at 20^o C), $P_r = 1.0$ (Prandtl number for electrolytic solution like salt water at 20^o C), $P_r = 7.0$ (Prandtl number correspond to water at 20^o C). The other parameters are taken arbitrarily.

To get the steady state solution of this developed model, the numerical computation has been carried out up to dimensionless time $\tau = 80.05$. But at the present case, changes appear till $\tau = 60$. And then onward the changes are not apparent. Therefore, $\tau = 60$ essentially represents steady state solution for this problem.

With the above mentioned parameters, the primary velocity profiles, the secondary velocity profiles as well as the temperature profiles has been expedited in Fig.2 to Fig.17. In Fig.2 the primary velocity caused affect due to different values of Magnetic parameter M. It has been depicted that as dimensionless magnetic parameter M increases the velocity profile decreases. So, it follows the boundary conditions. This decreasing occurs owing to the presence of magnetic field in the conducting fluid. The influence causes a resistive type of force called Lorentz force. This force has a tendency to slow down the lateral velocity. As expected the secondary velocity profiles increases with the increase of M which has been shown in Fig. 3. On the other hand, the temperature (are not shown for brevity) follows the interesting pattern. It is observed from Fig. 4, the primary velocity steeply increases with the increase of Hall current m. Thereafter the profiles have a tendency to meet the free stream velocity which satisfies the boundary conditions. The effects of Hall current m has also been expedited incase of secondary velocity in Fig. 5. The magnetic effect of thermal buoyancy force G_r on primary velocity has been shown in Fig. 6. It has been observed from the figure thatincreasing the values of the Grashof number G_r decreases in the primary velocity profiles. Also the secondary velocity profiles decreases with the increase of GrashofnumberG_r. In Fig. 8 the temperature increases for increasing values of G_r.

Various effects of dimensionless Eckert number E_c on different flow field are expedited in Figs. 9 to 10. It is interesting to note that as E_c increases, there is a rapid rise in the primary velocity near the surface of the vertical porous plate and then descends asymptotically to meet the free stream velocity. In Fig. 10, the temperature

profile increases near the plate and then onwards it tries to descend to get more stable as $E_c$increases. Fig. 11 has been shown to expedite various effects of Rotation parameter Γ on velocity flow field. It physically relates that the parameter decreases the fluid rotation and rotational boundary layer thickness. Also the secondary velocity decreases with the increase of Rotation parameter Γ as shown in Fig. 12.The effect of Prandlt number P_r on Primary velocity profile has been shown in Fig. 13. It has seen that the velocity profile decreases drastically for the increase of P_r. The effect of Prandlt number $P_r$causes fall of temperature at the same values of Prandltnumber P_r.Heat is therefore able to diffuse away more rapidly. In Fig.15 the effect of suction parameter ϵ on the primary velocity profile is noteworthy. For large suction the velocity profile decreases drastically whereas the secondary velocity increases severely with the increase of suction parameter ϵ. This is because sucking decelerates fluid particles through the wall reducing the growth of the boundary layer as well as thermal boundary layer as shown in Fig. 17.

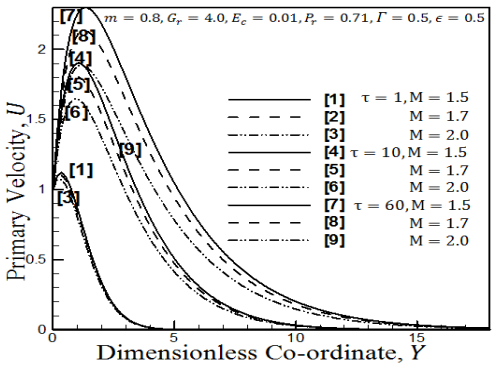

Fig. 2. Primary velocity profiles for dimensionless parameter M.

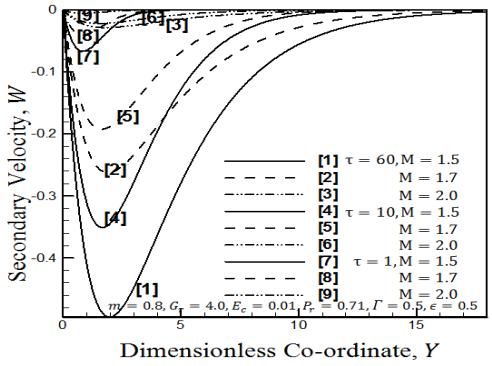

Fig. 3. Secondary velocity profiles for dimensionless parameter M.

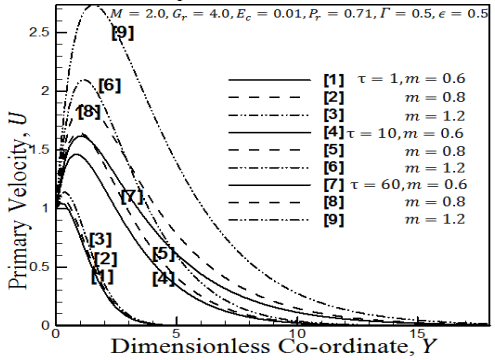

Fig. 4. Primary velocity profiles for dimensionless parameter m.

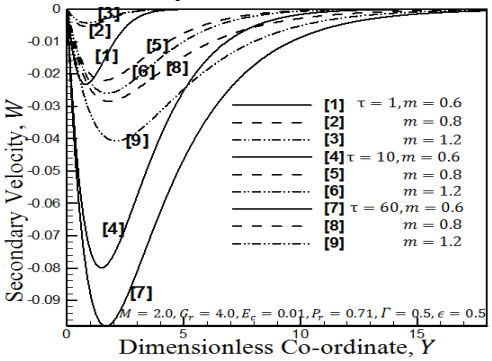

Fig. 5. Secondary velocity profiles for dimensionless parameter m.

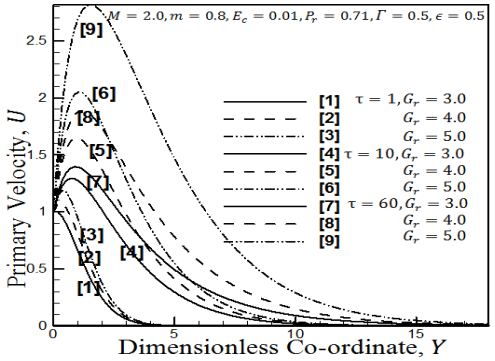

Fig. 6. Primary velocity profiles for dimensionless parameter G_r.

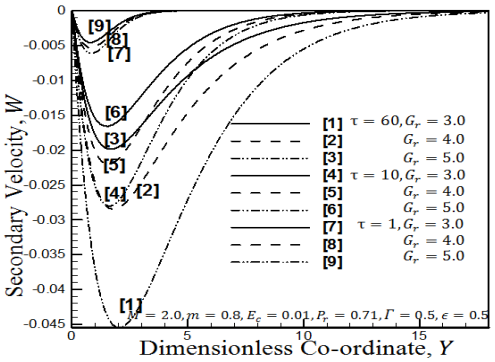

Fig.7. Secondary velocity profiles for dimensionless parameter G_r.

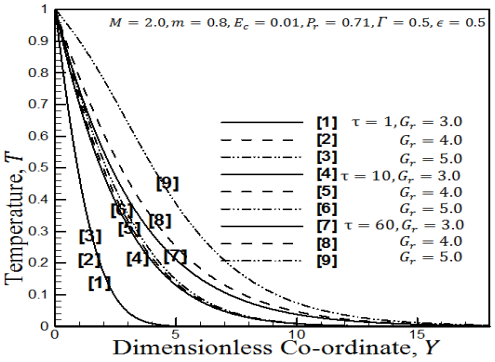

Fig. 8. Temperature for dimensionless parameter G_r.

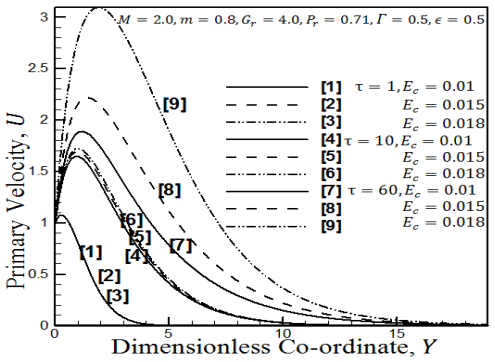

Fig. 9. Primary velocity profiles for dimensionless parameter E_c.

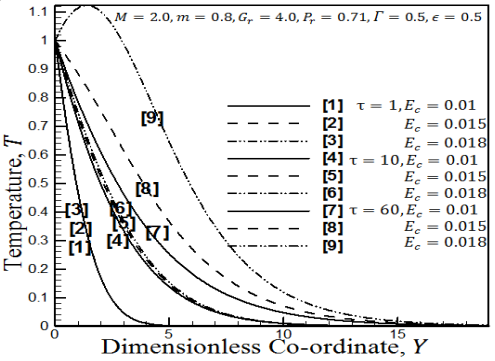

Fig. 10. Temperature for dimensionless parameter E_c.

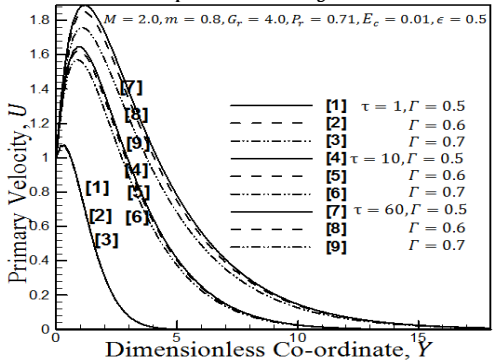

Fig. 11. Primary velocity profiles for dimensionless parameter Γ.

It is seen from Fig. 22 that, τ_x increases for the value $G_r \geq 1$.The Nusselt number $(-N_u)$ has fallen with the increase of Grashof numberG_r displayed in Fig.23. In Fig. 24, the shear stress τ_x increases with the increase of dimensionless Eckert number E_c. Nusselt number $(-N_u)$ fall with the increase of E_c as depicted in Fig. 25. Dimensionless Rotation parameter Γ resists the time development of shear stress in x-direction plotted in Fig. 26. But τ_z fall drastically with the increase of Rotation parameter as shown in Fig. 27.Different values of suction parameter S caused effects

on the shear stresses as shown in Fig. 28. Shear stress τ_x falls drastically for large suction. Indicating suction stabilizes the growth of the boundary layer. Negative Nusselt number $(-N_u)$ rises severely with the increase of suction has been expedited in Fig. 29.

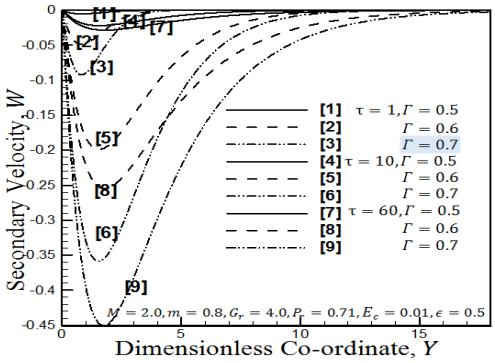

Fig.12. Secondary velocity profiles for dimensionless parameter Γ.

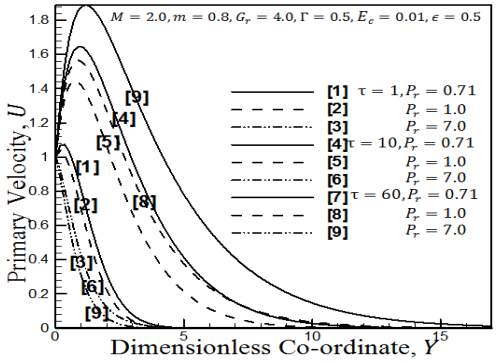

Fig.13. Primary velocity profiles for dimensionless parameter P_r.

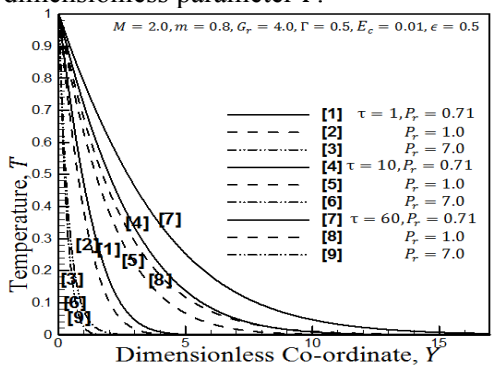

Fig. 14. Temperature for dimensionless parameter P_r.

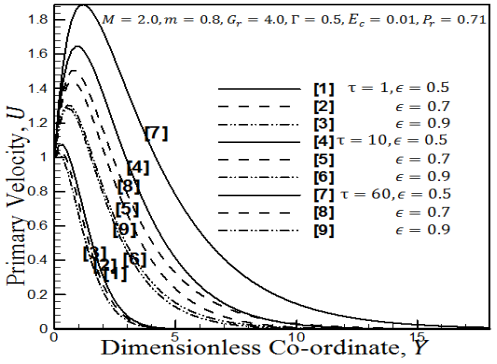

Fig. 15. Primary velocity profiles for dimensionless parameter ϵ.

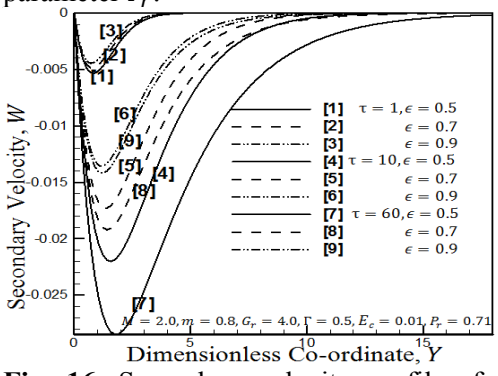

Fig. 16. Secondary velocity profiles for dimensionless parameter ϵ.

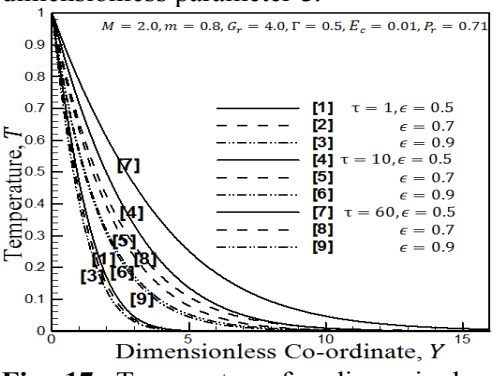

Fig. 17. Temperature for dimensionless parameter ϵ.

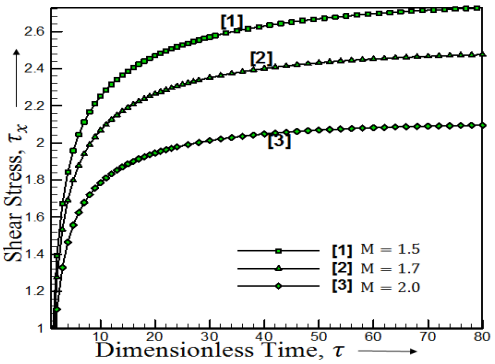

Fig.18. Shear Stress τ_x for dimensionless parameter M.

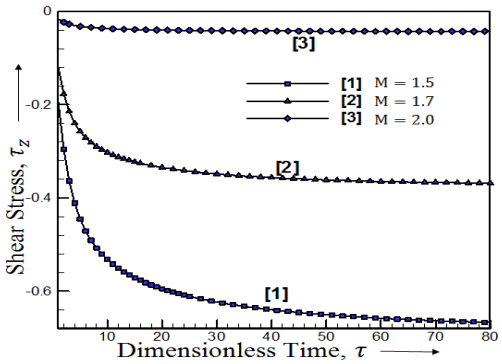

Fig.19. Shear Stress τ_z for dimensionless parameter M.

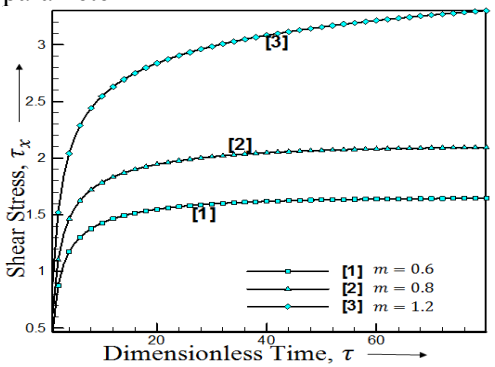

Fig. 20. Shear Stress τ_x for dimensionless parameter m.

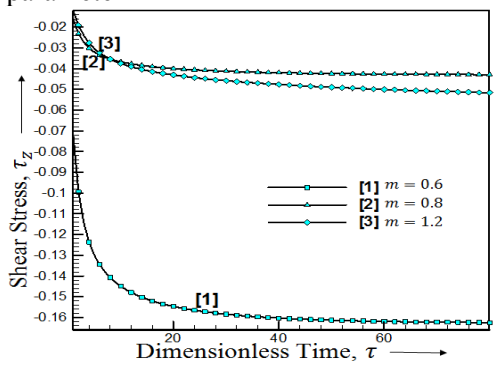

Fig. 21. Shear Stress τ_z for dimensionless parameter m.

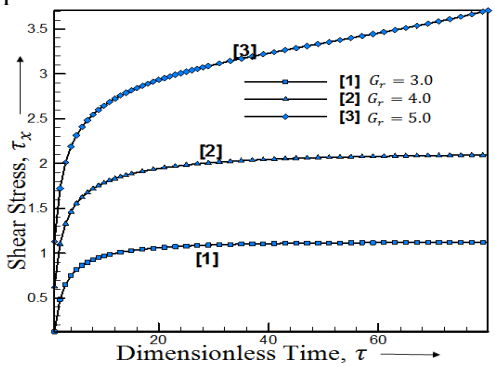

Fig. 22. Shear Stress τ_x for dimensionless parameter G_r.

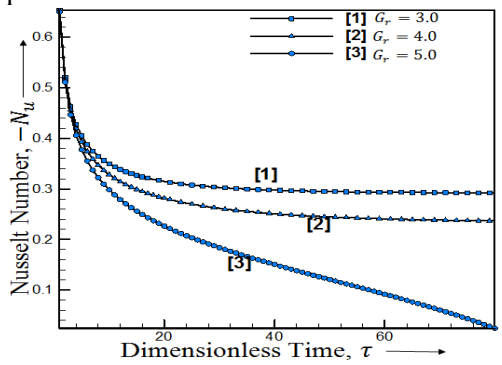

Fig. 23. Nusselt number $(-N_u)$ for dimensionless parameter G_r.

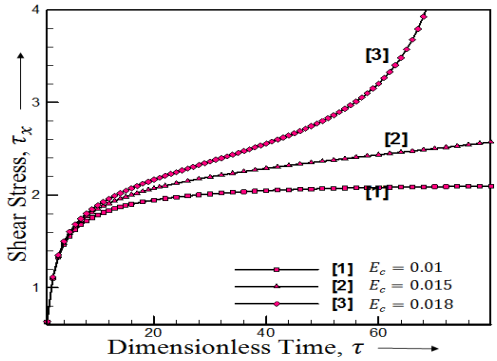

Fig. 24. Shear Stress τ_x for dimensionless parameter E_c.

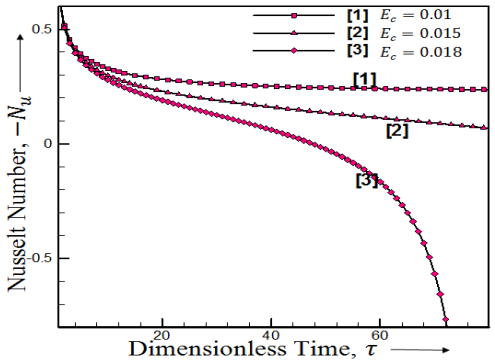

Fig. 25. Nusselt number $(-N_u)$ for dimensionless parameter E_c.

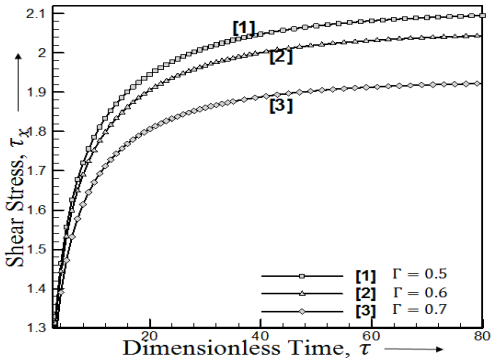

Fig. 26. Shear Stress τ_x for dimensionless parameter Γ.

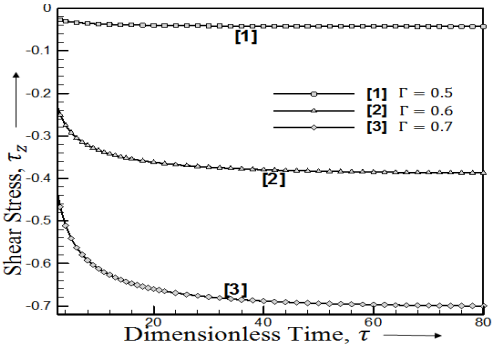

Fig. 27. Shear Stress τ_z for dimensionless parameter Γ.

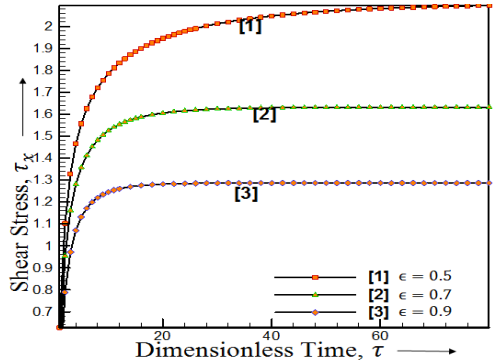

Fig. 28. Shear Stress τ_x for dimensionless parameter ϵ.

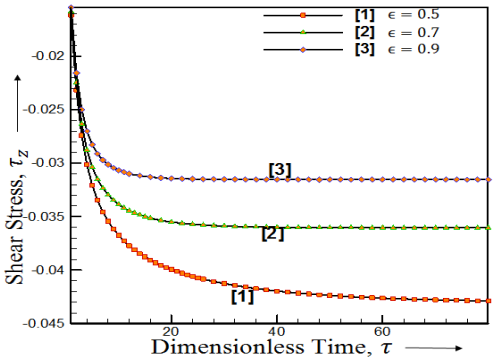

Fig. 29. Shear Stress τ_z for dimensionless parameter ϵ.

6. Conclusion

Hall current effects on unsteady MHD fluid flow past a porous vertical plate has been considered strong magnetic field. The resulting governing system of dimensionless coupled non-linear partial differential equations is numerically solved by an explicit finite

difference method. Some of the important findings obtained from the graphical representation of the results are listed below;

1. The primary velocity increases with the increase of m, G_r, E_c while it decreases with the increase of M, Γ, ϵ, P_r.
2. The secondary velocity increases with the increase of $M,\ m, P_r, \epsilon$ while it decreases with the increases of G_r, E_c, Γ.
3. The temperature increases with the increase of m, G_r, E_c, Γ while it decreases with the increases of P_r, M, ϵ.
4. The Nusselt number $(-N_u)$ increase with the increase of P_r, M, ϵ while it decreases with the increases of m, G_r, E_c, Γ.

The shear stressesτ_x, $\tau_z$follow the previous trends of Primary and Secondary velocities. The accuracy of present work is qualitatively good in case of all the flow parameters.

REFERENCES

1. E.M.Abo-Eldahaband E.M.E.Elbarbary, Hall current effect on magneto-hydrodynamic free convection flow past a semi-infinite vertical plate with mass transfer, *Int. J. Engg*. Sci., 39 (2001) 1641-1652.
2. M.M.Abdelkhalek, The skin friction in the MHD mixed convection stagnation point with mass transfer, *Int. commun Heat Mass*, 33 (2006), 249-258.
3. M.K.Chowdhury, M.N.Islam, MHD free convection flow of viscoelastic fluid past an infinite vertical porous plate, *Heat Mass transfer,* 36 (2000), 439-447.
4. L.J.Crane, Flow past a stretching sheet, *J. Appl. Math. Phys.,* 21 (1970), 645-647.
5. D. Pal and B. Talukdar, Buoyancy and chemical reaction effects on MHD mixed convection heat and mass transfer in a porous medium with thermal radiation and Ohmic heating, *Communications in Nonlinear Science and Numerical Simulation*, 15(10) (2010), 2878–2893.
6. K. E. Chin, R. Nazar, N. M. Arifin and I. Pop, Effect of variable viscosity on mixed convection boundary layer flow over a vertical surface embedded in a porous medium, *International Communications in Heat and Mass Transfer*, 34(4) (2007), 464–473.
7. M.A.Rana,A.M.Siddiquiand N.Ahmed, Hall effect on Hartmann flow and heat transfer of a Burger's fluid, *Phys. Letters A,* 372 (2008) 562-568.
8. S. Mukhopadhyay, Effect of thermal radiation on unsteady mixed convection flow and heat transfer over a porous stretching surface in porous medium, *International Journal of Heat and Mass Transfer*, 52(13-14) (2009),3261–3265.
9. T. Hayat, M. Mustafa, and I. Pop, Heat and mass transfer for Soret and Dufour's effect on mixed convection boundary layer flow over a stretching vertical surface in a porous medium filled with a viscoelastic fluid, *Communications in Nonlinear Science and Numerical Simulation*, 15(5) (2010), 1183–1196.